Open Access

OBM Genetics

LIDSEN Publishing Inc.

Original Research

Characterization of '*Ca*. Phytoplasma asteris', '*Ca*. Phytoplasma australiense' and '*Ca*. Phytoplasma mali' Associated with Russian Olive Witches'-Broom Disease in Iran Using Next-Generation Sequencing

Leila Zirak, Reza Khakvar *

Department of Plant Protection, Faculty of Agriculture, University of Tabriz, 5166616471, Tabriz, Iran; E-Mails: leilazirak@tabrizu.ac.ir; khakvar@tabrizu.ac.ir

* **Correspondence:** Reza Khakvar; E-Mail: khakvar@tabrizu.ac.ir

Academic Editor: Yuri Shavrukov

OBM Genetics
2023, volume 7, issue 4
doi:10.21926/obm.genet.2304204

Received: August 31, 2023
Accepted: November 29, 2023
Published: December 04, 2023

Abstract

Russian olive trees showing witches'-broom disease symptoms in urban green spaces and orchards in northwest Iran were sampled for phytoplasma detection. PCR assays and Sanger sequencing of 16S rRNA gene confirmed that '*Ca*. Phytoplasma asteris' was associated with Russian olive witches'-broom disease. For genomic characterization of phytoplasma associated with disease, the total DNA of an infected tree was analyzed by Illumina next-generation sequencing (NGS). The NGS analysis generated 46011389 read pairs of raw data with about 6.8×10^9 bp sequences and 31% GC content. Then, MetaPhlAn2 analysis of NGS raw data predicted three phytoplasma species inside the infected Russian olive tree DNA. Finally, the genomes of '*Ca*. Phytoplasma asteris' with 833199 bp length, '*Ca*. Phytoplasma australiense' with 762261 bp length and '*Ca*. Phytoplasma mali' with 518942 bp length were obtained from NGS raw data. This study represents the first report of '*Ca*. Phytoplasma australiense' and '*Ca*. Phytoplasma mali' association with Russian olive witches'-broom disease using NGS analyses worldwide.

Keywords

Russian olive witches'-broom; '*Ca*. Phytoplasma asteris'; '*Ca*. Phytoplasma australiense'; '*Ca*. Phytoplasma mali'; NGS; Iran

1. Introduction

Russian olive (*Elaeagnus angustifolia*) is a tree native to central and western Asia, especially Iran, growing wildly and cultivated in arid and semi-arid areas. The Russian olive tree is very tolerant to water shortage and has been developed in all water-scarce regions of Iran; accordingly, many artificial afforestation projects in Iran have been designed using the Russian olive as the main tree [1]. It is also resistant to many pests and diseases, so only a few Russian olive disorders have been reported in Iran [2].

The witches'-broom is the most important disease of the Russian olive, which is only reported from northwest Iran. However, it may be prevalent in other areas of the country. It was previously reported that the Russian olive witches'-broom disease is caused by '*Candidatus* Phytoplasma asteris' [3]. It was later revealed that the infected trees are a powerful source of phytoplasma transmission to other plants, especially stone fruits [4]. So far, no insect has been reported as a natural vector of the disease. However, leafhopper *Macropsis infuscata* (Hemiptera: Cicadellidae) was previously collected on infected trees and could be a potential vector of the disease [3].

In this research, we sequenced the whole genome of a Russian olive tree showing witches'-broom disease symptoms to characterize the causal agent of the disease. Results indicated that in addition to '*Ca.* Phytoplasma asteris', a few other phytoplasma species were associated with Russian olive witches'-broom disease, and infected trees are powerful sources of phytoplasma infection for other plants in northwest Iran.

2. Materials and Methods

2.1 Sampling and DNA Extraction

From July to September of six consecutive years, 2016 to 2021, urban green spaces, orchards, and artificial afforestation around Tabriz city located in East Azerbaijan province in the northwest of Iran were visited, and about 35 Russian olive trees showing witches'-broom symptoms were subjected to sampling (Figure 1). Total DNA extraction from approximately five grams of foliar tissues was performed following Murry and Thompson's protocol [5]. Extracted DNAs were solved in 100 µl distilled sterile water and stored at -20°C until use.

Figure 1 The Russian olive witches'-broom disease symptoms in Tabriz urban green space.

2.2 PCR Assays and Amplifications

For phytoplasma detection, PCR assays were done using phytoplasma universal primer pair P1/P7, which produces a 1784 bp 16S rRNA-encoding gene [6], followed by primer pair R16F2n/R16R2, which produces a 1239 bp 16S rRNA fragment in nested PCR [7]. In the first PCR, the reactions consisted of one cycle at 95°C for 5 min, 40 cycles at 95°C for 30 s, 50°C for 75 s, and 72°C for 90 s, and a final extension step at 72°C for 10 min. The total volume of 5 µl diluted (1:20) first PCR products was used as a template for nested PCR. For nested PCR, the condition was 94°C for 5 min, followed by 40 cycles at 94°C for 30 s, 50°C for 30 s, and 72°C for 45 s, and a final extension step at 72°C for 10 min.

The total volume of 15 µl PCR reaction mixture contained 5 µl of template DNA, 1 µl each of primer pairs (20 pmol), and 8 µl Amplicon *Taq* DNA Polymerase Master Mix RED (Ampliqon, Odense, Denmark). After amplification, each PCR product was electrophoresed with 1% agarose gel in 1x TAE buffer and stained with safe stain DNA Green Viewer. PCR bands were visualized in UV gel documentation (Figure 2).

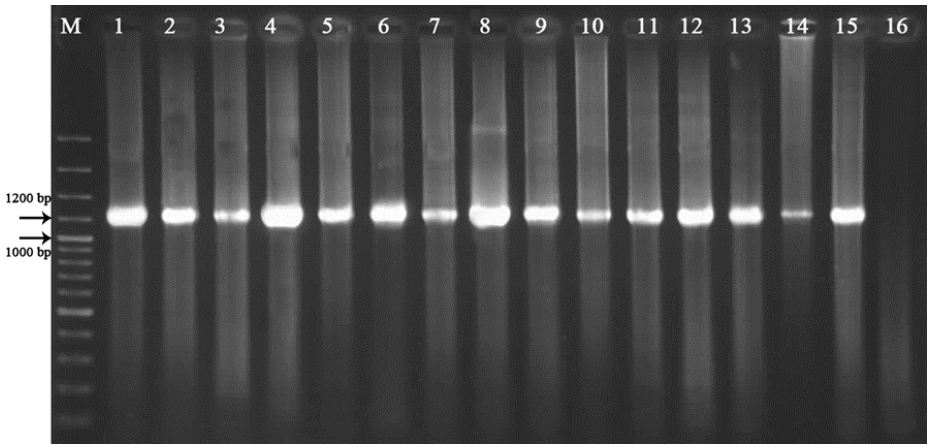

Figure 2 The 1239 bp phytoplasma 16S rRNA fragment was amplified in a nested PCR assay using the universal primer pair R16F2n/R16R2 from 15 symptomatic Russian olive trees. Lane 16 is the healthy tree as a negative control.

2.3 Sanger Sequencing of 16S rRNA

The 1239 bp fragments amplified in nested PCR using primer pair R16F2n/R16R2 were purified and sequenced directly by Microsynth company (Balgach, Switzerland). Then, the sequences were deposited into NCBI under accession numbers KJ920334 and MZ604438.

2.4 Next-Generation Sequencing (NGS) Analysis

For next-generation sequencing, about 100 µl of the DNA solution, with 5 µg/ml DNA extracted from tree foliage, was purified and used for library preparation. The concentration and purity of DNA was determined using a Qubit fluorometer. The qubit concentration of purified samples was 50 ng/µl and evaluated appropriately for the whole genome sequencing process. The Illumina 1.9 Novaseq 6000 platform generated a paired-end library in Novogene, China Company. Finally, about 6 GB of raw data was obtained.

2.5 Qualification and Profile of the Composition of Microbial Communities

The quality of Illumina raw data was checked by FastQC version 0.11.8 software [8]. Then, to profile microbial communities' structure and composition, the NGS raw data was analyzed with MetaPhlAn2 version 2.6.0 software [9]. According to MetaPhlAn2 prediction, three *'Ca*. Phytoplasma sp.' genomes existed inside NGS raw data (Table 1).

Table 1 The MetaPhlan2 analysis results for Russian olive tree NGS raw data.

Super-Kingdom	Phylum	Class	Species	% in NGS raw data
Bacteria	Tenericutes	Mollicutes	*'Ca.* P. asteris'	48.23863
			'Ca. P. australiense'	0.19511
			'Ca. P. mali'	0.06434
	Proteobacteria	Gammaproteobacteria		5.43987
		Betaproteobacteria		3.74242
		Alphaproteobacteria		0.27219
	Firmicutes	Clostridia		0.11394
	Bacteroidetes	Flavobacteriia		0.09308
	Actinobacteria	Actinobacteria		0.04013
Archaea	Euryarchaeota	Methanobacteria		0.00854
Viruses	Viruses no name	Viruses no name		40.72407
Eukaryota	Apicomplexa	Coccidia		0.3625
		Aconoidasida		0.05894
	Ascomycota	Saccharomycetes		0.30888
		Sordariomycetes		0.14944
		Schizosaccharomycetes		0.12313
		Eurotiomycetes		0.06479

2.6 Phytoplasma Genomes Preparation

For phytoplasma genome preparation, the NGS raw data was independently aligned to reference sequences created using genomes submitted to NCBI for phytoplasma genome construction using Bowtie2 version 2.4.2 software [10]. For first phytoplasma genome preparation, the NGS raw data was aligned to a reference genome of aster yellows witches'-broom phytoplasma AYWB (accession no. NC_007716) and its four plasmids including plasmids pAYWB-I (NC_007717), pAYWB-II (NC_007718), pAYWB-III (NC_007719) and pAYWB-IV (NC_007720) sequences. The *'Ca*. Phytoplasma australiense' genome (AM422018) and *'Ca*. Phytoplasma mali' genome (NC_011047) was independently utilized as a reference to align with NGS raw data for constructing the second and third phytoplasma genomes.

Following that, the aligned reads acquired for all three phytoplasmas were individually used for assembly analysis using metaSPAdes version 3.9.0.1 software [11]. The resulting contigs were clustered using CD-HIT-EST version 1.2 software [12]. Finally, the phytoplasma genomes at the contig level were deposited in the Genome database of NCBI, and PGAP annotation (NCBI Prokaryotic Genome Annotation Pipeline) was automatically done for each genome. The Assembly, BioSample, BioProject, WGS accession numbers, and genome NCBI-PGAP annotation results for all genomes are mentioned in Table 2.

Table 2 Genomic characteristics and PGAP analysis results of phytoplasmas associated with Russian olive witches' broom disease.

Features	*E. angustifolia* witches'-broom phytoplasma isolate TBZ1	'*Ca*. Phytoplasma mali' isolate Tabriz.1	'*Ca*. Phytoplasma australiense.' isolate Tabriz.2
Accession No.	JAHFWK010000000	JAKQYB000000000	JAINCS000000000
Assembly No.	GCA_018598675	GCA_022343605	GCA_019841745
BioSample No.	SAMN18826970	SAMN25756516	SAMN20931228
BioProject No.	PRJNA723969	PRJNA804530	PRJNA756976
Genome length (bp)	833199	518942	762261
Reference genome (bp)	723970	601943	879959
Contig number	1404	2052	2328
GC content (%)	26	22.5	24.5
Total Genes	557	479	775
Total CDSs	498	415	702
Coding Genes	477	411	683
CDSs with protein	477	411	683
Genes (RNA)	59	64	73
rRNAs	1, 11, 12 (5S, 16S, 23S)	1, 9, 21 (5S, 16S, 23S)	1, 13, 21 (5S, 16S, 23S)
complete rRNAs	1, 1 (5S, 16S)	1, 1, 1 (5S, 16S, 23S)	1, 1 (5S, 16S)
partial rRNAs	10, 12 (16S, 23S)	8, 20 (16S, 23S)	12, 21 (16S, 23S)

tRNAs	32	31	35
ncRNAs	3	2	3
Total Pseudo Genes	21	4	19
CDSs without protein	21	4	19
Pseudo Genes (ambiguous residues)	0 of 21	0 of 4	0 of 19
Pseudo Genes (frameshifted)	6 of 21	2 of 4	7 of 19
Pseudo Genes (incomplete)	14 of 21	2 of 4	11 of 19
Pseudo Genes (internal stop)	3 of 21	0 of 4	2 of 19
Pseudo Genes (multiple problems)	2 of 21	0	1 of 19

2.7 PCR Assays Using Group-Specific Primer Pairs

To assess the presence of '*Ca*. Phytoplasma mali' inside symptomatic trees DNA, primer pair AP3/AP4 group-specific primer pair to amplify non-ribosomal RNA region which produces 162 bp fragment [13], were used. The PCR condition was performed: 95°C for 5 min followed by 35 cycles at 95°C for 30 s, 57°C for 30 s, and 72°C for 30 s, and a final extension step at 72°C for 10 min. Also, to detect *'Ca*. Phytoplasma australiense' inside symptomatic tree DNA, primer pair R16F2n/R16R2 was used as nested PCR primer after the first PCR using primer pair R16F1/R16R0. PCR condition for primer pair R16F1/R16R0 was similar to primer pair P1/P7 [14].

3. Results

3.1 Phytoplasma Detection and Characterization

Russian olive trees showing witches'-broom disease symptoms were observed in the East Azerbaijan province for many years. In all areas, intense witches'-broom and little leaf symptoms appeared on the infected trees (Figure 1). The PCR assays using phytoplasma universal primer pairs indicated that in almost all DNA samples, the expected phytoplasma fragment was amplified (Figure 2). The Sanger sequencing of 16s rRNA gene from tree samples collected for consecutive years revealed that the '*Ca*. Phytoplasma asteris' was always associated with the infected trees.

3.2 Next-Generation Sequencing of Infected Trees' DNA

A symptomatic tree's DNA was subjected to next-generation sequencing using the Illumine platform for genomic characterization of phytoplasma associated with the disease. The length of raw data was 46011389 read pairs, and a totally of about 6.8×10^9 bp sequence was obtained. Each raw read length was 150 bp, and the insert size was 350 bp. The GC content of the whole genome was estimated at 31%.

3.3 Prediction of Phytoplasma Species Associated with Infected Tree

The NGS raw data was subjected to MetaPhlAn2 analysis to estimate the microbial populations associated with infected Russian olive trees. MetaPhlAn2 software predicted the taxonomic profile and microbial community of NGS raw data. The results indicated that, in addition to *'Ca*. Phytoplasma asteris' that is the accepted causal agent of Russian olive witches'-broom disease, two other phytoplasma genomes, including *'Ca*. Phytoplasma australiense' and *'Ca*. Phytoplasma mali' existed inside NGS raw data. Based on prediction analysis, about 99.5% of all phytoplasma populations inside symptomatic Russian olives belonged to the *'Ca*. Phytoplasma asteris,' whereas about 0.4% and 0.1% of the population belonged to *'Ca*. Phytoplasma australiense' and *'Ca*. Phytoplasma mali' respectively (Table 1).

3.4 Genomic Characterization of Phytoplasmas Associated with Russian Olive Witches'-Broom Disease

In previous studies, the *'Ca*. Phytoplasma asteris' was characterized as the causal agent of Russian olive witches 'broom disease in Iran [3, 15]. However, MetaPhlAn2 analysis suggested that, in addition to *'Ca*. Phytoplasma asteris', the genomes of *'Ca*. Phytoplasma australiense' and *'Ca*. Phytoplasma mali' were linked to the symptomatic Russian olive tree DNA.

To prepare *'Ca*. Phytoplasma mali' genome, the NGS raw data was aligned with a reference genome of *'Ca*. Phytoplasma mali', which was previously submitted in NCBI. Alignment results indicated that 0.1% of raw data sequences belonged to *'Ca*. Phytoplasma mali' genome. Assembly of aligned sequences resulted in a genome with 518942 bp size for the Iranian isolate of *'Ca*. Phytoplasma mali' (isolate Tabriz.1).

Also, to prepare *'Ca*. Phytoplasma australiense' genome, the NGS raw data was aligned to the reference genome of *'Ca*. Phytoplasma australiense' which was previously submitted to NCBI. The alignment results indicated that 0.4% of overall sequences in NGS raw data were aligned to *'Ca*. Phytoplasma australiense' reference genome. Assembly of aligned sequences resulted in a genome with 762261 bp size for the Iranian isolate of *'Ca*. Phytoplasma australiense' (isolate Tabriz.2).

3.5 Detection of 'Ca. Phytoplasma australiense' and 'Ca. Phytoplasma mali' Using PCR

After NGS analyses and predicting the presence of *'Ca*. Phytoplasma australiense' and *'Ca*. Phytoplasma mali' inside infected tree DNA, group-specific primer pairs belonging to apple proliferation group and *'Ca*. Phytoplasma australiense' were used for detection. However, no expected fragment was amplified in PCR using these specific primers.

4. Discussion

4.1 Russian Olive Witches'-Broom Disease Importance in the Northwest of Iran

The Russian olive is a tree native to Iran that grows wild and cultivated mainly in areas affected by drought stress. For many years, trees showing typical witches'-broom symptoms were observed in urban green spaces around Tabriz city and many orchards in northwest Iran. The disease has only been reported from northwest Iran so far (Figure 1). Later, the *'Ca*. Phytoplasma asteris' was

recognized, associated with the infected trees [3], and then the genome of Iranian *'Ca*. Phytoplasma asteris' was obtained using NGS analysis [15].

4.2 The 'Ca. Phytoplasma asteris' Pathogenicity in Iran

Among all phytoplasma species, the *'Ca*. Phytoplasma asteris' has the widest host range in Iran [16]. However, few trees have been reported to be infected by *'Ca*. Phytoplasma asteris' [4, 17-19]. Recently, almond, plum, and sweet cherry trees were found in stone fruit production areas in the northwest of Iran that were infected by *'Ca*. Phytoplasma asteris'. Russian olive trees showing witches'- broom were observed in the margin of affected stone fruit orchards. It seems that infected Russian olives are a rich source of phytoplasma in these areas, and possible effective insect vector(s) transmit the phytoplasma to neighbor stone fruit orchards [4].

The PCR results using universal primer pairs and Sanger sequencing of rRNA fragments indicated that *'Ca*. Phytoplasma asteris' was associated with infected trees, whereas NGS analysis showed that at least two other phytoplasma species were associated with the disease. But, any other phytoplasma could not be detected in PCR assays. It could be related to the low concentration of these phytoplasmas inside infected trees sap.

4.3 Next-Generation Sequencing and Several Phytoplasma Species Prediction

The NGS analysis of an infected Russian olive tree DNA resulted in 46011389 read pairs of raw data. The microbial population prediction results indicated that about 48.5% of the microbial population belonged to phytoplasmas, while 99.5% of the phytoplasma population belonged to the *'Ca*. Phytoplasma asteris' (48.2% of all microbial population) whereas only 0.4% of phytoplasma population belonged to *'Ca*. Phytoplasma australiense' (0.2% of all microbial population) and 0.1% of phytoplasma population belonged to *'Ca*. Phytoplasma mali' (0.06% of all microbial population). This phytoplasmas demographic composition justifies the reason why only *'Ca*. Phytoplasma asteris' is detected during PCR assays, and other phytoplasmas could not be seen because the population of other phytoplasma species is not high enough to be caught in PCR assays.

4.4 Genomic Characterization of Three Distinct Phytoplasma Species

The previously full genome of *'Ca*. Phytoplasma asteris' was obtained as the causal agent of Russian olive witches'-broom disease in Iran [15]. However, in this research, in addition to *'Ca*. Phytoplasma asteris', the genome of *'Ca*. Phytoplasma mali' was obtained as the second phytoplasma that could be involved in Russian olive witches'-broom disease. On the other hand, the *'Ca*. Phytoplasma australiense' was the third phytoplasma involved in Russian olive witches'-broom disease. There is not any report from *'Ca*. Phytoplasma australiense' and *'Ca*. Phytoplasma mali' detection in Iran at present time and this research is the first report of their association with Russian olive witches'-broom disease worldwide.

4.5 Phytoplasma Mixed Infected Diseases Prevalence Worldwide

Mix infection of two or more different phytoplasmas was limitedly reported. Mixed infection of phytoplasmas related to 16SrI-B and 16SrXII-A in lily plants [20], phytoplasmas related to aster yellows and elm yellows groups in jujube [21], phytoplasmas related to 16SrI-B, 16SrXII-A and

flavescence-dorée phytoplasma in grapevine [22] were limitedly reported based on PCR assays, 16S rRNA sequencing, actual and virtual RFLP analysis. However, as a result of present research, an association of three different phytoplasma species, including *'Ca*. Phytoplasma asteris', '*Ca*. Phytoplasma australiense' and *'Ca*. Phytoplasma mali' with Russian olive has been reported for the first time worldwide.

4.6 Next-Generation Sequencing Advantages in Detection of Phytoplasmas

Nowadays, several detection methods, such as PCR-based methods were used to phytoplasmas detection in plants. While applying these methods to phytoplasma detection, various difficulties are encountered. Also, PCR-based methods require the preparation of inaccurate DNA concentrations. On the other hand, all primers exhibit some homology to chloroplast DNA and other plant DNA [23]. As it was observed in this research, the *'Ca*. Phytoplasma asteris, which has a high population inside the trees, was usually amplified and detected, whereas other phytoplasmas present in low concentrations could not be detected using PCR.

The findings of this study demonstrated that by utilizing the NGS method, mixed infections of three distinct phytoplasma species, two of which had never been reported in Iran before, could be detected. The NGS is introduced as potentially an ideal, universal screening method for mixed infection disease diagnostics in plants. Identifying viruses using NGS-based approaches is feasible when viral disease symptoms are missing, unspecific, or caused by several viruses [24]. Therefore, as results obtained in this research indicate, the NGS method could be proposed as a susceptible and practical method in detecting mixed infection phytoplasma diseases in plants.

The Russian olive witches'-broom disease is a significant disease in northwest Iran. Previously, it was thought that the disease was caused solely by *'Ca*. Phytoplasma asteris', but this study discovered two other phytoplasma species, '*Ca*. Phytoplasma australiense' and *'Ca*. Phytoplasma mali' are involved in Russian olive witches'-broom disease, and infected Russian olive trees could be a powerful source of phytoplasma transmission to other plants. So far, no insect vectors or other disease transmission methods have been found, and identification of the insect vector(s) and other disease transmission methods is required for effective disease treatment.

Author Contributions

First author (Dr. Leila Zirak) has carried out most of the experiments and analysis and Dr. Reza Khakvar was supervisor for this project. All authors reviewed the manuscript.

Competing Interests

The authors have declared that no competing interests exist.

References

1. Tabatabaei M. Senjed = *Elaeagnus angustifolia* L (Elaeagnaceae) (In Persian). Tehran, Iran: SANA Publication; 2010. p. 92..
2. Ahmad Yousefi Sarhaddi F, Mohammadi M. First report of *Phellinus rimosus* as elm trees decline agent in Iran. Proceedings of the International Congress of Food Science and Technology, Agriculture and Food Security; 2020 September 21; Karaj, Iran. doi: 10.18502/jfqhc.7.1.2444.

3. Hajizadeh A, Khakvar R, Bashir NS, Zirak L. Detection of Russian olive witches'-broom disease and its insect vector in Northwestern Iran. J Plant Prot Res. 2017; 57: 309-313.
4. Zirak L, Khakvar R, Zarrini G, Hasanpour K. Detection and molecular characterization of phytoplasmas associated with stone fruit trees in northwest of Iran. Crop Prot. 2021; 142: 105526.
5. Murray MG, Thompson WF. Rapid isolation of high molecular weight plant DNA. Nucleic Acids Res. 1980; 8: 4321-4326.
6. Schneider B, Marcone C, Kampmann M, Ragozzino A, Lederer W, Cousin MT, et al. Characterization and classification of phytoplasmas from wild and cultivated plants by RFLP and sequence analysis of ribosomal DNA. Eur J Plant Pathol. 1997; 103: 675-686.
7. Lee IM, Hammond RW, Davis RE, Gundersen DE. Universal amplification and analysis of pathogen 16S rDNA for classification and identification of mycoplasmalike organisms. Phytopathology. 1993; 83: 834-842.
8. Brown J, Pirrung M, McCue LA. FQC dashboard: Integrates FastQC results into a web-based, interactive, and extensible FASTQ quality control tool. Bioinformatics. 2017; 33: 3137-3139.
9. Truong DT, Franzosa EA, Tickle TL, Scholz M, Weingart G, Pasolli E, et al. MetaPhlAn2 for enhanced metagenomic taxonomic profiling. Nat Methods. 2015; 12: 902-903.
10. Langmead B, Salzberg SL. Fast gapped-read alignment with Bowtie 2. Nat Methods. 2012; 9: 357-359.
11. Bankevich A, Nurk S, Antipov D, Gurevich AA, Dvorkin M, Kulikov AS, et al. SPAdes: A new genome assembly algorithm and its applications to single-cell sequencing. J Comput Biol. 2012; 19: 455-477.
12. Fu L, Niu B, Zhu Z, Wu S, Li W. CD-HIT: Accelerated for clustering the next-generation sequencing data. Bioinformatics. 2012; 28: 3150-3152.
13. Jarausch W, Saillard C, Dosba F, Bové JM. Differentiation of mycoplasmalike organisms (MLOs) in European fruit trees by PCR using specific primers derived from the sequence of a chromosomal fragment of the apple proliferation MLO. Appl Environ Microbiol. 1994; 60: 2916-2923.
14. Davis RE, Dally EL, Gundersen DE, Lee IM, Habili N. "*Candidatus* Phytoplasma australiense," a new phytoplasma taxon associated with Australian grapevine yellows. Int J Syst Bacteriol. 1997; 47: 262-269.
15. Azizpour N, Nematollahi S, Khakvar R, Jamshidi M, Norouzi Beirami MH. Identification of endophytic microbiota of phytoplasma-infected Russian olive trees "*Elaeagnus Angustifolia* L." in the Northwest of Iran. Forests. 2022; 13: 1684.
16. Sichani FV, Bahar M, Zirak L. Characterization of phytoplasmas related to aster yellows group infecting annual plants in Iran, based on the studies of 16S rRNA and *rp* genes. J Plant Prot Res. 2014; 54: 1-8. doi: 10.2478/jppr-2014-0001.
17. Zirak L, Bahar M, Ahoonmanesh A. Characterization of phytoplasmas related to '*Candidatus* Phytoplasma asteris' and peanut WB group associated with sweet cherry diseases in Iran. J Phytopathol. 2010; 158: 63-65.
18. Hashemi Tameh M, Bahar M, Zirak L. '*Candidatus* Phytoplasma asteris' and '*Candidatus* Phytoplasma aurantifolia', new phytoplasma species infecting apple trees in Iran. J Phytopathol. 2014; 162: 472-480.

19. Hashemi Tameh M, Bahar M, Zirak L. Molecular characterization of phytoplasmas related to apple proliferation and aster yellows groups associated with pear decline disease in Iran. J Phytopathol. 2014; 162: 660-669.
20. Bertaccini A, Botti S, Martini M, Kaminska M. Molecular evidence for mixed phytoplasma infection in lily plants. Acta Hortic. 2002; 568: 35-41.
21. Lee SH, Han SS, Cha BJ. Mixed infection of 16S rDNA I and V groups of phytoplasma in a single jujube tree. Plant Pathol J. 2009; 25: 21-25.
22. Marzachi C, Boarino A, Vischi A, Palermo S, Morone C, Loria A, et al. Single and mixed infection by phytoplasmas of three 16S ribosomal subgroups (IB: Aster yellows, VC: Flavescence doree and XIIA: Stolbur) in grapevines of southeastern Piemonte. Informatore Fitopatologico. 2001; 51: 58-63.
23. Heinrich M, Botti S, Caprara L, Arthofer W, Strommer S, Hanzer V, et al. Improved detection methods for fruit tree phytoplasmas. Plant Mol Biol Rep. 2001; 19: 169-179.
24. Jones S, Baizan Edge A, MacFarlane S, Torrance L. Viral diagnostics in plants using next generation sequencing: Computational analysis in practice. Front Plant Sci. 2017; 8: 1770.